Journal of Radiation Research, Vol. 60, No. 2, 2019, pp. 178–188
doi: 10.1093/jrr/rry099
Advance Access Publication: 8 January 2019

The radiobiological effects of He, C and Ne ions as a function of LET on various glioblastoma cell lines

Ming Tsuey Chew[1,*], David A. Bradley[1,2], Masao Suzuki[3], Naruhiro Matsufuji[4], Takeshi Murakami[5], Bleddyn Jones[6] and Andrew Nisbet[2,7]

[1]Sunway University, School of Healthcare and Health Sciences, Centre for Biomedical Physics, No. 5, Jalan Universiti, Bandar Sunway, 47500 Petaling Jaya, Selangor, Malaysia
[2]Department of Physics, Faculty of Engineering and Physical Sciences, University of Surrey, Guildford, GU2 7XH, UK
[3]Department of Basic Medical Sciences for Radiation Damages; National Institute of Radiological Sciences (NIRS), National Institutes for Quantum and Radiological Science and Technology, 4-9-1 Anagawa, Inage-ku, Chiba-shi, Chiba 263-8555, Japan
[4]Radiation Effect Research Team, Department of Accelerator and Medical Physics, NIRS, National Institutes for Quantum and Radiological Science and Technology, 4-9-1 Anagawa, Inage-ku, Chiba-shi, Chiba 263-8555, Japan
[5]Heavy-Ion Radiotherapy Promotion Unit & Department of Accelerator and Medical Physics, NIRS, National Institutes for Quantum and Radiological Science and Technology, 4-9-1 Anagawa, Inage-ku, Chiba-shi, Chiba, 263-8555, Japan
[6]Gray Laboratory, CRUK/MRC Oxford, Oncology Institute, University of Oxford, ORCRB-Roosevelt Drive, Oxford OX3 7DQ, UK
[7]The Department of Medical Physics, Royal Surrey County Hospital, Egerton Road, Guildford, GU2 7XX, UK
*Corresponding author. Sunway University, School of Healthcare and Health Sciences, Centre for Biomedical Physics, No. 5, Jalan Universiti, Bandar Sunway, 47500 Petaling Jaya, Selangor, Malaysia. Tel: +603-7491-8622 ext. 7447; Fax: +603-5635-8633; Email: mtchew@sunway.edu.my
(Received 17 April 2018; revised 7 August 2018; editorial decision 22 October 2018)

ABSTRACT

The effects of the charged ion species ^{4}He, ^{12}C and ^{20}Ne on glioblastoma multiforme (GBM) T98G, U87 and LN18 cell lines were compared with the effects of 200 kVp X-rays (1.7 keV/μm). These cell lines have different genetic profiles. Individual GBM relative biological effectiveness (RBE) was estimated in two ways: the RBE_{10} at 10% survival fraction and the $RBE_{2\ Gy}$ after 2 Gy doses. The linear quadratic model radiosensitivity parameters α and β and the α/β ratio of each ion type were determined as a function of LET. Mono-energetic ^{4}He, ^{12}C and ^{20}Ne ions were generated by the Heavy Ion Medical Accelerator at the National Institute of Radiological Sciences in Chiba, Japan. Colony-formation assays were used to evaluate the survival fractions. The LET of the various ions used ranged from 2.3 to 100 keV/μm (covering the depth–dose plateau region to clinically relevant LET at the Bragg peak). For U87 and LN18, the RBE_{10} increased with LET and peaked at 85 keV/μm, whereas T98G peaked at 100 keV/μm. All three GBM α parameters peaked at 100 keV/μm. There is a statistically significant difference between the three GBM RBE_{10} values, except at 100 keV/μm ($P < 0.01$), and a statistically significant difference between the α values of the GBM cell lines, except at 85 and 100 keV/μm. The biological response varied depending on the GBM cell lines and on the ions used.

Keywords: GBM; ^{12}C ions; ^{20}Ne ions; ^{4}He ions; LET

INTRODUCTION

Glioblastoma multiforme (GBM), a Grade IV malignant astrocytic glioma, is the most common subtype and the most lethal form of primary brain tumour [1]. GBM has the hallmarks of uncontrolled cellular proliferation, diffuse infiltration, propensity for necrosis (and hypoxia), robust angiogenesis, intense resistance to apoptosis and extensive heterogeneous genomic instability [2]. For these reasons, it is difficult to treat GBM successfully. The standard of care for GBM is surgical resection, where possible, and radiotherapy with concomitant Temozolomide [3]. Radiotherapy has been a key treatment for GBM, and conventional radiotherapy consists of 60 Gy of external beam irradiation delivered 5 days per week in fractions of 1.8–2.0 Gy [4, 5]. However, 90% of GBMs usually recur near the original site or within the high-dose region [4–6] after standard radiotherapy treatment. Dose escalation to

70–80 Gy can achieve local control, but relapse then occurs elsewhere in the brain. The prognostic factors for GBM are World Health Organization (WHO) classification, age of patient, tumour location, neurologic performance status, extent of surgical resection, proliferative indices, and genetic alterations [7].

The Cancer Genome Atlas (TCGA) studied GBM as its first cancer type. TCGA aims to catalogue and discover major cancer-causing genome alterations in large cohorts of human tumours through integrated multidimensional analysis. It aims to establish this feasibility and has the power to rapidly expand our knowledge of the molecular basis of cancer and the patterns of mutation that may inform future therapeutic decisions, thus setting the stage for a new era in the discovery of cancer interventions [8]. Besides phenotypes, genotypes of the central nervous system tumours also play an important role in the effective treatment of GBM, such that Louis *et al.* [9] have incorporated molecular parameters into the 2016 WHO classification of tumours in the central nervous system, including GBMs, with the objective of improved diagnostic accuracy, as well as improved patient management and more accurate determination of prognosis and treatment response. Halperin has predicted, in his historical review of particle therapy and treatment of cancer, that insights into molecular biology might clarify the ideal particles for clinical situations [10]. In addition, Van Meir *et al.* [5] propose that, due to each individual GBM tumour's uniqueness in its expression profile, personalized medicine may be indicated for defined therapies and homogenous responses for critical subgroups.

Although conventional radiotherapy has been the mainstay in treatment for GBM, it is one of the most radioresistant tumours due to its persistently hypoxic nature, its ability to repair radiation-induced injury (which is accomplished by aberrant/or amplified growth), and survival signalling pathways [5, 11], as well as changes in the phosphatase and tensin homolog (*PTEN*) and *p53*, both tumour suppressor genes that have been linked to radioresistance [5, 12–15].

Charged particle/ion radiotherapy potentially possesses physical and biological advantages over photons (megavoltage X-rays). The physical benefits of heavy, charged particles provided by the Bragg peak allow precise delivery of high radiation doses to tumours while minimizing destructive irradiation to normal tissues and critical organs at risk. Furthermore, its depth–dose distributions can be modulated/shaped (by means of the 'spread-out Bragg peak') to cover tumours of different shapes, and the increase in ion density Linear Energy Transfer (LET) [16] can also make it a potentially superior modality of radiation compared with photons. Increasing LET (within the clinical range) increases the Relative Biological Effectiveness (RBE), reduces the Oxygen Enhancement Ratio (OER), produces less variation in cell-cycle–related radiosensitivity and decreases the ability to repair radiation damage [17]. RBE is dependent on many factors, such as cell and tissue type, biological end point, culture condition, dose, dose rate and fractionation, charged particle type, LET, and oxygenation status [18, 19].

Numerous basic *in vitro* cellular studies on GBM cell lines using photons [20–24] and various heavy ions [25–30] have been carried out. Pilot Phase I and II clinical studies using heavy ions such as helium, neon and carbon ions have been undertaken with the aim of improving radiotherapy for GBM patients [31–38].

Treating GBM with neon ions was first investigated by Castro *et al.* [32] with 14 GBM patients, and an optimal prescribed dose was not demonstrated, except that there was a trend toward better results with higher doses. Further work could not be done, because the Berkeley accelerator was shut down for budgetary reasons.

Carbon ion radiotherapy has been made available in Japan at the National Institute of Radiological Science (NIRS) since June 1994. Since the successful report of carbon ion radiotherapy by Tsujii *et al.* from NIRS using the Heavy Ion Medical Accelerator (HIMAC) [39], much attention has been focused on carbon ions. The first GBM Phase I–II trials using carbon ion as a boost for treatment has been reported as successful by Mizoe *et al.* [34], but unfortunately it did not proceed to a Phase III clinical trial. It should be noted that the RBE used was 3. Combs *et al.* [37, 38] have reported two randomized Phase II trials to evaluate the use of carbon ion radiotherapy as a boost versus a proton boost for primary GBM patients after surgery and standard chemotherapy with Temozolomide; and using carbon ion versus fractionated stereotactic radiotherapy in patients with recurrent or progressive gliomas.

Due to its invasive, highly infiltrative nature and heterogeneous genetic alteration properties, GBM is known to be one of the most resistant cancers to aggressive multimodality treatments. Moreover, past GBM clinical trials with carbon and neon ion radiotherapy have not attained optimum effectiveness [32, 34]. The key aim of this study was to answer the question: is the same charged ion therapy effective for all GBM patients? To seek to answer this question, it was decided to estimate the RBE_{10} and $RBE_{2\ Gy}$, α, β and α/β ratio for each individual GBM cell type. The response of these GBM cell types to ^{4}He, ^{12}C and ^{20}Ne ions as a function of LET and dose was investigated. To our knowledge, this is one of the first studies to use three different GBM cell lines with various charged ions and various LETs for each ion. Recent studies in the literature have mostly concentrated on other cell lines [40–44].

MATERIALS AND METHODS

Cell lines and cell maintenance

Three Grade IV GBM cell lines: T98G, U87 and LN18, with different genetic alterations, doubling times and morphologies were used,

Table 1. Characteristics of the established glioblastoma cell lines employed

Cell	*p53* status/genotype	*PTEN*	Doubling time	Morphology
T98G	Mutated/homozygous	Mutated	22 ± 3 h	Fibroblastic
U87	Wild type/homozygous	Mutated	35 ± 4 h	Epithelial
LN18	Mutated/heterozygous	Wild	33 ± 4 h	Epithelial

as shown in Table 1. The T98G cells were a gift from Mick Woodcock, Gray Institute for Radiation Oncology and Biology, Oxford, UK; the U87 cells were obtained from the Health Protection Agency Culture Collections (HPACC, Wiltshire, UK), and the LN18 cells were obtained from the American Type Culture Collection (ATCC, Middlesex, UK). All the cell lines were confirmed *Mycoplasma* free with a Lonza MycoAlert® Mycoplasma Detection Assay.

Cell lines were maintained in 75 cm^3 plastic flasks (T75 BD FalconTM 353084) in Eagle's Minimum Essential Medium (MEM: Nissui Pharmaceutical Co. Ltd, Tokyo) supplemented with 10% fetal bovine serum (FBS: Hyclone, Thermo Scientific, USA) in a humidified 95% air/5% CO_2 incubator at 37°C. Cells were subcultured from a T75 plastic flask by rinsing in calcium- and magnesium-free phosphate-buffered saline (PBS), and exposed to 0.2% Trypsin solution containing 0.5 mM EDTA. Cell numbers were determined by Coulter Counter. For all experiments, 3×10^5 cells of each cell line were inoculated into a 25 cm^3 plastic flask (T25 BD Falcon 353014) 3 days before irradiation to enable the cells to be at approximately 85–90% confluent stage for all dose points.

Irradiation

Cells were irradiated with ^4H, ^{12}C and ^{20}Ne monochromatic ion beams accelerated by the HIMAC, Japan. The energy and dose average LET for each of the various ions used are shown in Table 2. Lucite absorbers with various thickness were used to change the energy/LET of the beams. The details of the HIMAC beam delivery system, physical characteristics, biological irradiation procedures and dosimetry have been described by Kanai *et al.* and Torikoshi *et al.* [45, 46]. The dose average LET values range from 1.7 to 100 keV/μm, as shown in Table 2. The dose rate of all ion beams used was ~3 Gy/min. A 200 kVp X-ray (20 mA) beam filtered with 0.5 mm Cu and 0.5 mm Al by a TITAN 320 irradiator (Ge Inspection Technologies Shimadzu, Japan) at a dose rate of 1.00 Gy/min ± 0.02 was used as the reference radiation. All the irradiations were carried out at room temperature. Two or more independent experiments were performed with each ion species and LET, except for ^4He and ^{20}Ne (30 keV/μm) for LN18, for which only one experiment was performed, and no ^4He experiments were carried out for U87 due to beam line unavailability. For dose calculation, fragmentations were taken into consideration and applied to convert particle fluence (Φ) to dose, as described in Suzuki *et al.* and Matsufuji *et al.* [27, 47]:

$$\text{Dose(Gy)} = 1.6021 \times 10^{-9} \times \text{LET(keV/μm)} \times \Phi(\text{cm}^{-2}) \quad (1)$$

Cell-survival assay

Cell inactivation was measured with the colony-formation assay to assess reproductive death. After irradiation, cells were removed from the T25 flask, and appropriate numbers were inoculated into triplicate 60 mm plastic dishes (Falcon 353002) to produce 60–70 colonies per dish. Cells were counted using a Coulter Counter (Coulter Electronics Ltd, Japan, Tokyo). The plating efficiency (PE) for T98G is 0.46 ± 0.007, for U87 0.15 ± 0.002, and for LN18 it is 0.95 ± 0.03, with the stated uncertainty showing the standard error of the mean (SEM). Although U87 has a PE of only 0.15, irradiation with doses of up to 4 Gy still produced ~40 colonies at a LET of 85–100 keV/μm. Fourteen days later, colonies were washed, fixed and stained with 0.2% crystal violet. Triplicate dishes of each dose point colony (consisting of >50 cells) were counted under a stereomicroscope. The surviving fraction (SF) of each dose was determined as the ratio of live colonies in the treated dish relative to the untreated/control dish. The mean values and standard deviations of triplicate samples were calculated.

Data and statistical analysis

Surviving fraction data were obtained from the mean of at least two or more independent experiments and fitted by the least squares Linear Quadratic (LQ) Model equation:

$$S = \exp(-\alpha D - \beta D^2), \quad (2)$$

where S is the surviving fraction and D is the dose in gray. Doses were calculated from particle fluence and the LET values, as shown in Equation 1. The parameters α and β are constants describing the linear component and the quadratic part of the curve, respectively. The α and β parameters are determined by minimizing the sum of squares calculated by Equation 2. It is known that there is an almost linear relationship between the high-LET charged particle dose and cell killing for higher doses. However, the linear equation was not used to fit the survival curves due to the inherent low-dose hyper-radiosensitivity (HRS) of some GBM species [21, 22, 48]. Furthermore, low doses of 0.2, 0.25, 0.4, 0.5, 0.6 and 0.75 Gy were used to detect low-dose HRS of GBM cell lines. The highest dose used was 8 Gy for LET ≤85 keV/μm.

RBE is defined as the ratio of a reference photon dose D_γ and a corresponding ion dose D_I yielding the same biological effect:

$$RBE_{10} = D_\gamma / D_I \quad (3)$$

RBE_{10} is the dose ratio at a surviving fraction of 10% for X-rays relative to each ion.

$RBE_{2\ Gy}$ is the ratio of the surviving fraction at 2 Gy for X-rays in relation to each ion. $RBE_{2\ Gy}$ is of particular interest, because some strains of GBM are known to exhibit low-dose HRS after single low doses [21, 22, 48]. Moreover, most of the fractionated doses given clinically are between 1.8 and 2 Gy.

The α/β ratio is the dose, in Gy, when the number of cells killed by the linear component is equal to the cell kill from the quadratic component in the linear quadratic equation. The survival curves versus LET were plotted with KaleidaGraph by Synergy software (version 3.5). Analysis of variance (ANOVA) of the mean value of α and RBE_{10} values for each individual GBM cell line and ion were analysed using Xcel ANOVA for a single factor (Analysis Tool-kit). *P* values of <0.01 were considered significant.

RESULTS

A summary of all the GBM results with the various ions at different energies and LETs are shown in Table 2. Uncertainties in LET are expressed as the SEM, with uncertainties for all other parameters expressed as the standard deviation (SD).

Table 2. Summary of the GBM cell lines' α, β, α/β ratio, D_{10}, RBE_{10}, $RBE_{2\ Gy}$ and the ratio of $RBE_{2\ Gy}/RBE_{10}$ fitted into the LQ model

Cell lines		T98G—*p53* mutation homozygous and *PTEN* mutation							
Energy MeV/n	LET keV/μm	α (Gy^{-1})	β (Gy^{-2})	α/β (Gy)	D_{10} (Gy)	RBE D_{10}	$D_{2\ Gy}$ SF ratio	RBE 2 Gy	Ratio of RBE $D_{2\ Gy}/D_{10}$
200 kVp	1.70 ± 0.02	0.049 ± 0.001	0.109 ± 0.009	0.45	4.57 ± 0.023	1.00 ± 0.050	0.588 ± 0.021	1.00 ± 0.035	1.00
^{4}He 150	2.30 ± 0.04	0.045 ± 0.001	0.116 ± 0.001	0.39	4.63 ± 0.026	1.00 ± 0.006	0.579 ± 0.004	1.02 ± 0.007	1.02
^{4}He 150	13.0 ± 0.05	0.141 ± 0.004	0.104 ± 0.003	1.36	4.09 ± 0.045	1.12 ± 0.013	0.500 ± 0.007	1.18 ± 0.017	1.05
^{12}C 290	13.3 ± 0.19	0.201 ± 0.002	0.053 ± 0.004	3.79	5.21 ± 0.006	0.88 ± 0.001	0.541 ± 0.009	1.09 ± 0.019	1.24
^{20}Ne 400	30.0 ± 0.45	0.292 ± 0.001	0.141 ± 0.008	2.07	3.14 ± 0.065	1.46 ± 0.030	0.318 ± 0.010	1.85 ± 0.056	1.27
^{12}C 290	85.0 ± 0.32	0.643 ± 0.009	0.075 ± 0.003	8.57	2.71 ± 0.008	1.69 ± 0.005	0.204 ± 0.002	2.88 ± 0.023	1.70
^{20}Ne 400	85.0 ± 0.25	0.885 ± 0.007	0.042 ± 0.001	21.1	2.35 ± 0.006	1.95 ± 0.005	0.144 ± 0.001	4.08 ± 0.042	2.09
^{12}C 135	100 ± 1.77	0.935 ± 0.010	0.025 ± 0.004	37.4	2.32 ± 0.003	1.97 ± 0.002	0.140 ± 0.000	4.20 ± 0.021	2.13
Cell lines		U87—*p53* wild type and *PTEN* mutation							
Energy MeV/n	LET keV/μm	α (Gy^{-1})	β (Gy^{-2})	α/β (Gy)	D_{10} (Gy)	RBE D_{10}	$D_{2\ Gy}$ SF ratio	RBE 2 Gy	Ratio of RBE $D_{2\ Gy}/D_{10}$
200 kVp	1.70 ± 0.02	0.157 ± 0.006	0.068 ± 0.004	2.31	4.81 ± 0.078	1.00 ± 0.016	0.559 ± 0.002	1.00 ± 0.005	1.00
^{4}He 150	2.30 ± 0.04	N/A	N/A	N/A	N/A	N/A	NA	NA	NA
^{4}He 150	13.0 ± 0.05	N/A	N/A	N/A	N/A	N/A	NA	NA	NA
^{12}C 290	13.3 ± 0.19	0.315 ± 0.001	0.071 ± 0.002	4.44	3.90 ± 0.040	1.23 ± 0.013	0.401 ± 0.004	1.39 ± 0.014	1.13
^{20}Ne 400	30.0 ± 0.45	0.596 ± 0.004	0.029 ± 0.001	20.6	3.31 ± 0.009	1.45 ± 0.004	0.269 ± 0.001	2.08 ± 0.001	1.43
^{12}C 290	85.0 ± 0.32	0.774 ± 0.006	0.111 ± 0.001	6.97	2.25 ± 0.050	2.14 ± 0.048	0.136 ± 0.005	4.11 ± 0.146	1.92
^{20}Ne 400	85.0 ± 0.25	0.913 ± 0.010	0.003 ± 0.001	304	2.53 ± 0.035	1.90 ± 0.026	0.160 ± 0.003	3.49 ± 0.059	1.84
^{12}C 135	100 ± 1.77	1.102 ± 0.101	0.039 ± 0.038	28.3	2.27 ± 0.034	2.12 ± 0.032	0.100 ± 0.034	5.59 ± 0.065	2.64

Cell lines		LN18—*p53* mutation heterozygous and *PTEN* wild type							
Energy MeV/n	LET keV/µm	α (Gy^{-1})	β (Gy^{-2})	α/β (Gy)	D_{10} (Gy)	RBE D_{10}	$D_{2\ Gy}$ SF ratio	RBE 2 Gy	Ratio of RBE $D_{2\ Gy}/D_{10}$
200 kVp	1.70 ± 0.02	0.316 ± 0.001	0.076 ± 0.001	4.16	3.81 ± 0.010	1.00 ± 0.004	0.392 ± 0.002	1.00 ± 0.001	1.00
^{4}He 150	2.30 ± 0.04	0.271 ± 0.000	0.038 ± 0.000	7.13	4.98 ± 0.000	0.76 ± 0.000	0.499 ± 0.000	0.79 ± 0.000	1.04
^{4}He 150	13.0 ± 0.05	0.374 ± 0.000	0.038 ± 0.000	9.84	4.29 ± 0.000	0.89 ± 0.000	0.406 ± 0.001	0.97 ± 0.001	1.09
^{12}C 290	13.3 ± 0.19	0.277 ± 0.003	0.075 ± 0.001	3.69	4.00 ± 0.010	0.95 ± 0.003	0.426 ± 0.004	0.92 ± 0.008	0.97
^{20}Ne 400	30.0 ± 0.45	0.543 ± 0.000	0.061 ± 0.000	8.90	3.14 ± 0.000	1.21 ± 0.000	0.265 ± 0.000	1.48 ± 0.000	1.22
^{12}C 290	85.0 ± 0.32	0.853 ± 0.014	0.227 ± 0.004	3.76	1.80 ± 0.001	2.11 ± 0.005	0.073 ± 0.001	5.37 ± 0.063	2.53
^{20}Ne 400	85.0 ± 0.25	0.936 ± 0.031	0.039 ± 0.003	24.0	2.25 ± 0.050	1.70 ± 0.037	0.132 ± 0.007	2.97 ± 0.149	1.75
^{12}C 135	100 ± 1.77	1.079 ± 0.002	0.052 ± 0.001	20.8	1.95 ± 0.001	1.95 ± 0.002	0.094 ± 0.001	4.17 ± 0.007	2.14

NA = not available, SF = surviving fraction. Errors indicate standard error of the mean.

D_{10} is the dose required to inactivate the cells to 10% survival.

RBE_{10} and $RBE_{2\ Gy}$ and the $RBE_{2\ Gy}/RBE_{10}$ ratio and a comparison of the effects of genetic mutation of GBM are presented in Table 2. Figures 1–3 show survival curves of X-rays (1.7 keV/µm) and ions (up to 100 keV/µm). Figure 1A compares the radiosensitivity of the three GBM cell lines to X-rays, Fig. 1B compares their radiosensitivity to ^{12}C ions (13.3 keV/µm), and Fig. 1C compares their radiosensitivity to ^{20}Ne (entrance LET of 30 keV/µm). Figure 2 compares T98G and LN18 with ^{4}He ions at 2.3 and 13 keV/µm, respectively. Figure 3 compares ^{12}C (85 and 100 keV/µm) and ^{20}Ne ions (85 keV/µm). Figure 4 demonstrates T98G, U87 and LN18 trends for α and RBE_{10} in relation to LET, and Fig. 5 the β parameters as a function of LET.

Table 2 shows the RBE_{10} values of T98G relative to X-rays, ranging from 0.88 to 1.97. The α values ranged from 0.045 to 0.935. The T98G α and RBE_{10} values increased with LET (Figs 1–4). There was no discernible trend for β values (Fig. 5). The α/β values ranged from 0.39 to 37.4. The α/β values for high LET of ^{20}Ne and ^{12}C, with values of 21.1 and 37.4 respectively, have been highlighted to show the large increase when compared against C, Ne and He ion beams of low LET. Doses of 2 Gy produced higher RBE (Table 2), and $RBE_{2\ Gy}$ ranged from 1.02 to 4.20 (Table 2). The ratio of $RBE_{2\ Gy}$ to RBE_{10} was 1.02 to 2.13. RBE plays an important role in the treatment of patients, because it directly affects the resulting biological damage from radiation, and the common RBE used is at 10% survival. $RBE_{2\ Gy}$ is of interest because the clinically fractionated doses given were mostly between 1.8 and 2 Gy. Fertil and Malaise have reported that 2 Gy irradiation could provide valuable information and is a good indicator for intrinsic tumour cell radiosensitivity to photon radiation [49].

U87's RBE_{10} values ranged from 1.23 to 2.14 (Table 2), and increased with LET up to 85 keV/µm. U87 α and RBE_{10} values showed a trend of progressively increasing with ion mass and LET. The increase in α was prominent and consistent, but β values of U87 did not increase with LET and heavier ion mass (Figs 4 and 5). U87 α/β values ranged from 2.31 to 304 (Table 2). The $RBE_{2\ Gy}$ ranged from 1.39 to 5.59, and the ratio of $RBE_{2\ Gy}$ to RBE_{10} ranged from 1.13 to 2.64 (Table 2).

LN18 RBE_{10} values ranged from 0.76 to 2.11 (Table 2). There was a trend of LN18 α and RBE_{10} values increasing with LET and ion mass (Fig. 4). The β values did not show any consistent trend (Fig. 5). α/β values above 20 are seen for LET ≥85 keV/µm. The $RBE_{2\ Gy}$ of LN18 ranged from 0.79 to 5.37, and the ratio of $RBE_{2\ Gy}$ to RBE_{10} ranged from 0.97 to 2.53. Only with LN18 was there a lower than unity ratio of $RBE_{2\ Gy}$ to RBE_{10} (Table 2).

The results demonstrate that treatment of GBM could be ion specific with respect to effective cell killing. For example, for cell line LN18, ^{12}C ions at 85 keV/µm were observed to be the most effective ion for cell inactivation. In contrast, ^{20}Ne ions were more effective for T98 inactivation. The most effective LET for U87 and LN18 was that of the ^{12}C ion at 85 keV/µm. Conversely, the ^{12}C ions at 100 keV/µm did not increase cell inactivation, measured in terms of D_{10} survival; indeed, the reverse was true. ^{12}C ions at LET of 100 keV/µm were more effective for the cell line T98G, and ^{20}Ne ions at LET of 85 keV/µm were also effective for T98G (Table 2). The LET of the ^{4}He ions at 2.3 and 13 keV/µm was considered to be too low for any significant inactivation of GBM cells.

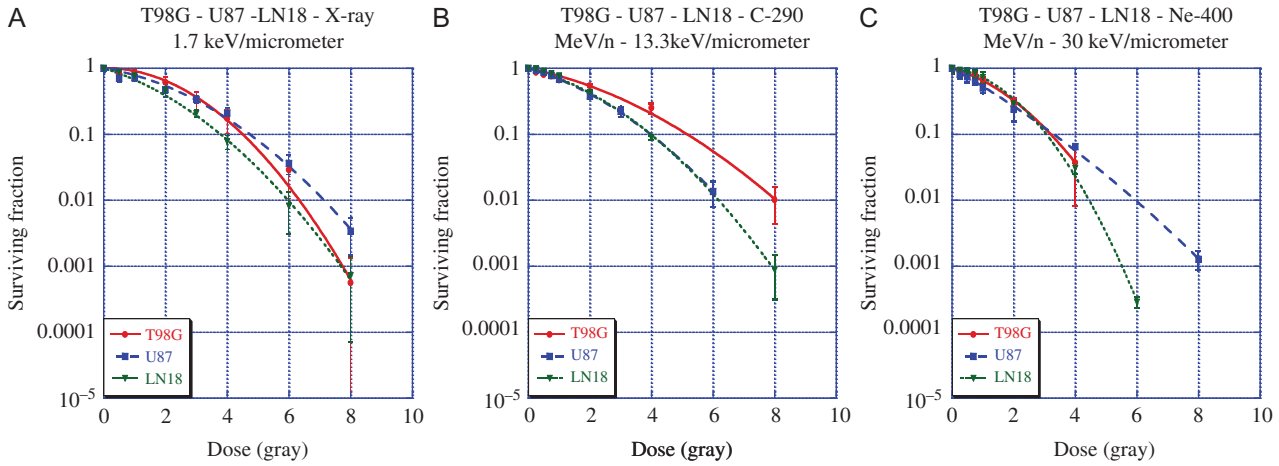

Fig. 1. Survival curves of T98G-U87-LN18 with (A) X-rays (1.7 keV/µm), (B) ^{12}C 290 MeV/n (13.3 keV/µm) and (C) ^{20}Ne 400 MeV/n (30 keV/µm). Error bars indicate standard deviations.

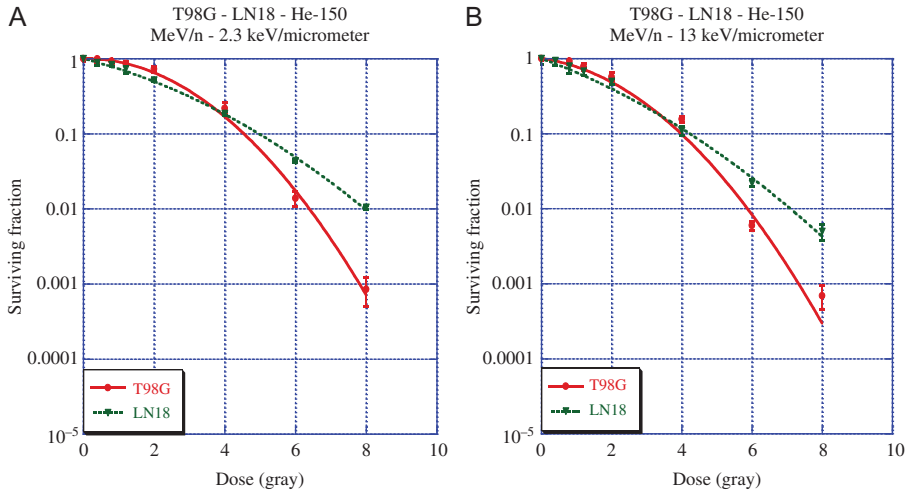

Fig. 2. Survival curves of T98G and LN18 with ^{4}He 150 MeV/n (A) at 2.3 keV/µm and (B) at 13 keV/µm. LN18 is more radioresistant than T98G. Error bars indicate standard deviations.

However, due to limited beam time availability, ^{4}He experiments were not conducted for U87.

The difference between the mean each of the GBM α-values has statistical significance ($P < 0.01$), except for that for ^{20}Ne ions (LET 85 keV/µm) and ^{12}C ions (LET 100 keV/µm); and between the mean RBE_{10}, except for ^{12}C ions (LET 100 keV/µm).

DISCUSSION

The charged ion irradiations to the three GBM cell lines resulted in a range of biological effectiveness. The responses of these GBM cell types to ^{4}He, ^{12}C and ^{20}Ne as a function of LET and dose also differed from one GBM type to the other. The results for RBE_{10} versus $RBE_{2\ Gy}$, RBE_{10} as a function of LET, α and β versus LET; comparison of previously reported data using GBM tumour cells, and the GBM genotype characteristics are discussed below.

RBE_{10} and $RBE_{2\ Gy}$

The RBE values of ions are relevant for treatment planning as they are used to calculate the Gy Equivalent dose (GyE). However, this is dependent on many factors, leading to further uncertainties. The classic RBE is conservatively taken from D_{10}, but the RBE at $D_{2\ Gy}$ may need to be considered because the doses given to patients are conventionally 1.8–2 Gy per fraction. From Table 2, $RBE_{2\ Gy}$ for U87 peaks at 100 keV/µm, and RBE_{10} for U87 peaks at 85 keV/µm. For LN18, the RBE_{10} and $RBE_{2\ Gy}$ both peak at 85 keV/µm. The U87 and LN18 RBE_{10} were not in agreement with reported RBE_{10} peak values at 100–200 keV/µm [40, 41, 50]. These differences in RBE values could be related to the repair capacity of the cells [51]. There was a trend for RBE_{10} and $RBE_{2\ Gy}$ to increase with LET, and for T98G the RBE_{10} reported here may not reflect the true peak measured RBE because the maximum LET used was 100 keV/µm [52, 53].

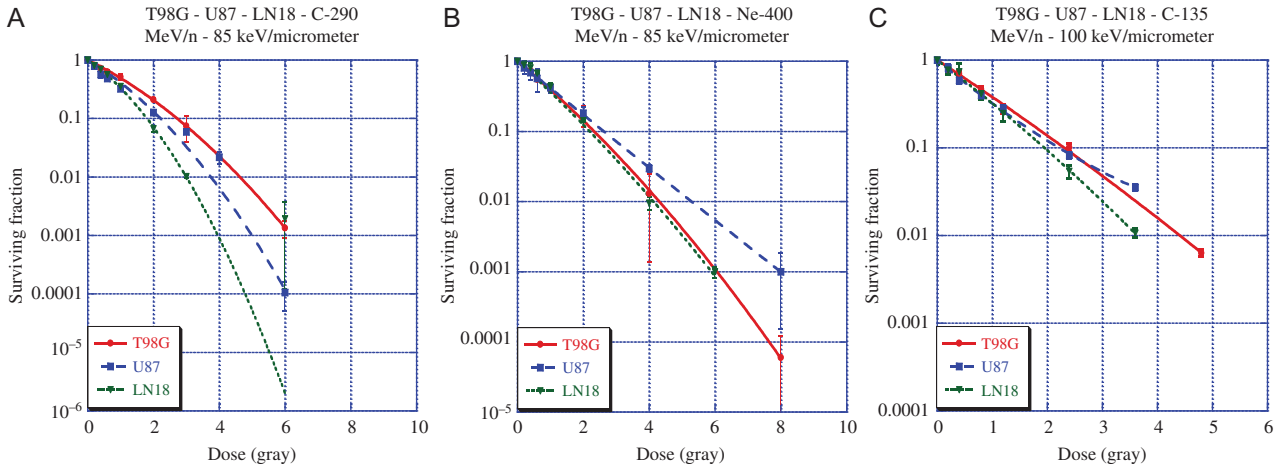

Fig. 3. (A and B) Survival curves comparing LETs of 85 keV/µm of ^{12}C 290 MeV/n and ^{20}Ne 400 MeV/n, respectively, and (C) ^{12}C 135 MeV/n (100 keV/µm). LN18 is more radiosensitive and T98G more radioresistant to ^{12}C (85 and 100 keV/µm). U87 is more radioresistant to ^{20}Ne (85 keV/µm). Error bars indicate standard deviations.

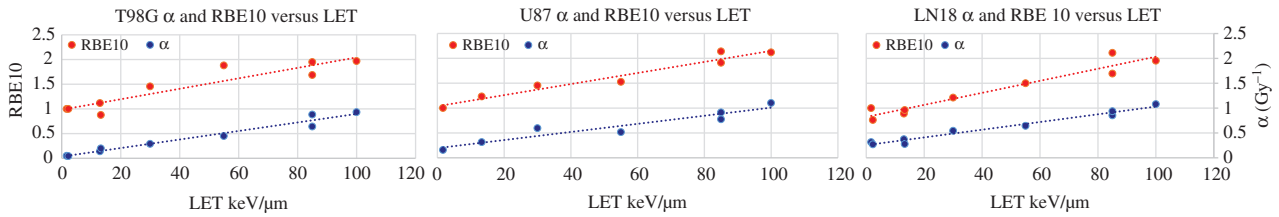

Fig. 4. Comparison of trends for T98G, U87 and LN18 α parameters and RBE$_{10}$ as a function of LET.

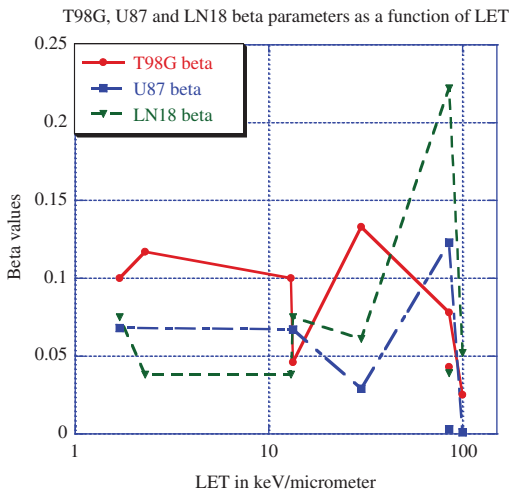

Fig. 5. T98G, U87 and LN18 β parameters as a function of LET.

However, our results do concur with previous reports in that different ions with different energies but the same LET had different RBE$_{10}$, as shown by the results for ^{20}Ne and ^{12}C-ions with LET of 85 keV/µm (Table 2 and Fig. 3) [50]. Our results were also in agreement with Tobias *et al.* [54] in that RBE$_{10}$ was dependent on cell type, because each individual GBM cell line studied had a different genetic alteration. The intrinsic and genetic alterations of the GBM cells may be the parameters that determine the radiosensitivity. In general, there is a trend for RBE$_{10}$ to increase with the *Z* values of ions. RBE is dependent on many factors and could be selected from D_{10}, D_{37} or D_1 [17]; $D_{2\ Gy}$ may also need to be considered, because the clinical doses given to patients are typically 1.8–2 Gy per fraction. Moreover, RBE$_{2\ Gy}$ is important, because some strains of GBM exhibit low dose HRS [20, 21]. Using RBE$_{10}$ alone may miss the intrinsic and inherent subtle nature of some strains of this tumour. It has been reported that 2 Gy irradiations provide the most valuable information and could be a good indicator for intrinsic tumour cell radiosensitivity to photon radiation [49]. The RBE was higher with $D_{2\ Gy}$, and the $D_{2\ Gy}/D_{10}$ ratio could demonstrate (infer) the radiobiological effectiveness of the respective ions and LET at 2 Gy; and may indicate the potential ion of choice. From both RBE$_{10}$ and RBE$_{2\ Gy}$, there is an inference that, for LET values of 85 keV/µm, ^{20}Ne ions (85 keV/µm) are appropriate for T98G; and ^{12}C ions (85 keV/µm) are more effective for both U87 and LN18 (Fig. 3A and B; Table 2). In addition to RBE$_{2\ Gy}$ and its ratio to RBE$_{10}$; the ratio of plateau to Bragg peak LET may be significant; for example, with T98G, ^{12}C (LET 13.3 keV/µm) had a RBE$_{10}$ of 0.88, and for ^{12}C (LET 85 keV/µm) the RBE$_{10}$ was 1.69. The plateau to Bragg peak ratio was therefore 1.92. For U87, the ratio was

1.74 (2.14/1.23), and for LN18 2.22 (2.11/0.95). This suggests that the RBE along the entire depth–dose curve should be taken into consideration.

RBE as a function of LET

The trend of RBE increasing with LET was observed in the T98G cell line, but not for U87 or LN18. U87 and LN18 RBE_{10} peaked at ^{12}C (LET 85 keV/μm), and an increase in LET to 100 keV/μm resulted in lower RBE (Fig. 4). The results show that higher LET did not equate to higher RBE for these GBM cell lines. The true peak RBE for T98G was not ascertained, because the maximum LET studied here was 100 keV/μm. Since the LET range studied was limited, it would not be appropriate to plot the RBE as a function of Z^{*2}/v^2 (where Z^* is the effective charge and v is the relative velocity of the ion) instead of LET [55]. Further work using an appropriate extended range of LET may be warranted.

α, β and LET

The α value characterizes the linear component of cell kill in the linear quadratic equation. The results show there was a trend of α increasing for LET up to 100 keV/μm (Fig. 4). This is in agreement with Hall and Giaccia, that the optimal LET for producing a biological effect is 100 keV/μm [17]. At this density of ionization, the average separation between ionizing events approximately coincides with the 2 nm diameter width of a DNA double helix and has the highest probability of causing a double-strand break by a single charged particle. There are also ion-kill and delta ray (equivalent to low-LET) effects, which lead to variation in radiosensitivity with LET [55]. There was a trend for T98G to be more radioresistant than U87 and LN18 with low LET. However, this trend was not observed with high LET, where the type of ion used was the dominant factor in determining radiosensitivity. The β values did not show any trend (Fig. 5).

Comparison with previously reported results

Comparing our results with others, the T98G α and β values for X-rays reported by Suzuki *et al.* (0.064/0.046) differed to some extent from those in this report (0.049/0.109). Also, for the ^{12}C ion (LET 13.3 keV/μm), our results (0.201/0.053) differed from Suzuki *et al.*'s (0.127/0.065), as did those for the ^{12}C ion (LET 77 keV/μm versus 85 keV/μm) (0.432/0.0895 versus 0.643/0.075). This could be due to the different dose rates: for X-rays 0.85 Gy/min vs 1.0 Gy/min, and for ^{12}C ions 1.2 Gy/min vs 3.0 Gy/min [27]. U87 and LN18 have increased radiosensitivity to ^{12}C ions compared with ^{20}Ne ions at the same LET of 85 keV/μm, which concurs with the results of Suzuki *et al.*, who reported that ^{12}C ions are more effective at the same LET [42] for mutation frequency/yield. In addition, it has been suggested that beams of different ion species could cause different types of DNA damage [56]; different ion species with different structures of energy deposition may cause qualitatively different damages, even with the same LET [42], and a difference in the track structure of the core and penumbra exist for different kinds of ions with similar LET [57]. Our results were also in agreement with those of Short *et al.*, that T98G and U87 exhibited HRS to X-ray irradiation [20, 21]. Short *et al.* state that HRS usually occurs at doses of <1 Gy with X-rays; our slightly different results could be due to our dose rate of 1 Gy/min (as compared with that of Short *et al.*, 0.2–0.4 Gy/min). Furthermore, the methods and medium employed were different. Low-dose HRS is common in radioresistant glioma and is more marked in more radioresistant cell lines [21]. There is an inference that treating GBM with high fractionated doses for both low- and high-LET radiation may not be beneficial for all GBM cell lines.

Comparing ^{12}C ion irradiation of U87 by Combs *et al.* [29], despite the different setting, materials and methods (X-ray dose rates of 2.3 versus 1 Gy/min and ^{12}C ions with a LET of 103 versus 100 keV/μm), irradiation method (active raster-scanning techniques versus passively delivered ^{12}C ions) and media used, the results varied only slightly in α values: X-rays 0.176 versus 0.157, ^{12}C ions RBE_{α} 4.77 versus 7.0 and ^{12}C ion RBE_{10} 2.38 versus 2.12.

GBM genotypes

GBM has the hallmark of extensive genomic instability [2] and is known to be radioresistant to conventional X-ray therapy. However, T98G is one of the strains of GBM that demonstrate HRS to doses of <1 Gy but radioresistance to high doses [20]. It has been suggested that inducible repair processes are important components of radioresistance apparent in these cells at high doses [20]. The genotypes of GBM are directly related to radioresistance. *p53* and *PTEN* mutations are two known genetic alterations of GBM [4, 58]. Mutated *p53* is known to be involved in radioresistance to photons and charged ion radiations. Carbon ion irradiations can potentially overcome this resistance due to their high LET [25]. *PTEN* (on chromosome 10) and *p53* are both tumour suppressor genes that have been linked to radioresistance [5, 12–15]. Therefore, GBM cell lines with wild-type *p53* and *PTEN* will be more radiosensitive than the GBM cell lines with mutated *p53* and *PTEN*. Moreover, the severity of the mutations also plays an important part (heterozygous or homozygous). From the genotypes of the GBM studied, namely, T98G (*p53* homozygous mutated and *PTEN* mutated), U87 (*p53* wild-type homozygous and *PTEN* mutated) and LN18 (*p53* heterozygous mutated and wild-type *PTEN*), the expectation would be that T98G would be the most radioresistant, U87 would be of intermediate resistance and LN18 would be the least radioresistant.

U87 has homozygous wild-type *p53* and *PTEN* mutation, whereas LN18 has *p53* heterozygous mutation and wild-type *PTEN*, and they both have *p53* wild type (one or two alleles). Wild-type *p53* tumour suppressor is a key mediator of an ATM-dependent DNA damage response cascade following cellular exposure to ionizing radiation. Mutated *p53* can give rise to alteration in G1 and G2 cell-cycle checkpoint control, cell death, DNA repair, and genetic stability. As T98G has homozygous mutated *p53*, they will be expected to be more radioresistant as compared with U87 and LN18.

Although, both U87 and T98G have mutated *PTEN*, they were not compared, because it has been found that the *PTEN* locus revealed a *p53* binding element directly upstream of the *PTEN* gene in the regulation of PTEN transcription by p53 [15], and that

PTEN was required for *p53*-mediated apoptosis and demonstrates a functional interaction between these two genes [15]. Since T98G has both mutated *p53* and *PTEN*, the expectation is that they will be more radioresistant.

Our U87 and LN18 results have demonstrated that wild-type *p53* cell lines (homozygous or heterozygous) are not radioresistant to ^{12}C ions with high LET (85–100 keV/μm). In contrast, T98G, with mutated *p53* (homozygous), exhibits generally lower α values, an indication of resistance (Table 2).

Another observable classification of GBM cell lines can be based on ion specificity, showing that U87 and LN18 cell lines are more sensitive to ^{12}C than to ^{20}Ne (Fig. 1B and Fig. 3A). Conversely, T98G is more radiosensitive to ^{20}Ne ions (Fig. 1C and Fig. 3B). LN18 is radioresistant to ^{4}He ions at high doses, but is radiosensitive to low doses, and the reverse is true for T98G. The survival curves (Fig. 2A and B) are not equal in size: B is smaller than A.

Due to the genetic differences between these tumours, it has been suggested that individual predictive assays (and tailored treatments) may prove beneficial for defining growth parameters and determining inherent radiosensitivity suited to high-LET therapy [31]. Probably, with charged ion radiation, eligibility criteria may be essential for the benefit of patients [59], as has been demonstrated for tumours in patients with 1p and 19q co-deletion, which are sensitive to chemotherapy with procarbazine, lomustine and vincristine. The status of chromosomes 1p and 19q are now used as eligibility criteria, rather than histologic assessment [4]. With this precedent, it may be necessary for a paradigm shift in stratifying genetic alteration in the design of clinical trials for GBM patients using charged particle radiotherapy.

There was a statistically significant difference ($P < 0.01$) between the mean RBE_{10} (except for LET 100 keV/μm) and α value [except for ^{20}Ne ions (LET 85 keV/μm) and ^{12}C ions (LET 100 keV/μm)]. There is evidence that personalized charged ion radiotherapy is indicated for GBM patients [5, 10, 31]. Moreover, there is ion specificity for GBMs, as it was shown for U87 and LN18 cell lines that ^{12}C was more effective at inactivation than ^{20}Ne, whereas the T98G cell line was more radiosensitive to ^{20}Ne ions. It was demonstrated that individual GBM cell types responded differently to the same LET and same charged ion radiation. The genotypes of GBM are likely to be directly associated with radiosensitivity and radioresistance, because there was a statistically significant difference between the determined α values and RBE_{10} parameters. The influence of the choice of ion, energy and treatment dose on the benefits for GBM patients may have to be considered. It may be necessary to stratify GBM genetic alteration in the design of future clinical trials for GBM patients using charged ion radiotherapy, rather than only using the histopathological GBM types.

In conclusion, the individual GBM cell types respond differently to the same LET and same charged ion radiation. The statistically significant difference ($P < 0.01$) between the mean RBE_{10} (except for LET 100 keV/μm) and the α value [except for ^{20}Ne ions (LET 85 keV/μm) and ^{12}C ions (LET 100 keV/μm)] infer that the same charged ion therapy may not be effective for all GBM types. In addition, the genotypes of GBM may also be contributory factors to effective treatment of GBM.

Future work on GBM response to ^{12}C and ^{20}Ne ions using a wider range of LET for each ion species (with its unique *Z* value) is necessary in order to determine the maximum value of RBE, because this study could not determine the true maximum value of RBE. Of interest is also the effect of hypoxic conditions, with a LET of 85 keV/μm possibly providing a better understanding of the hypoxic tumour response to charged ion radiation. There is also a need to investigate the capacity of GBM cells to repair after ion irradiation.

ACKNOWLEDGEMENTS

We thank the engineering staff of HIMAC for their help with all the ion beam irradiations performed. We also thank Dr Annelie Meijer, who introduced University of Surrey to NIRS/HIMAC, Chiba, Japan, and acknowledge the technical support and assistance of Drs CH Liu, M Wada and N Autsavapromporn.

CONFLICT OF INTEREST

The authors declare that there is no conflict of interest.

FUNDING

This work was supported in part by the International Open Laboratory NIRS and by NIRS/HIMAC; and was fully funded by the PARTNER of the European Commission, FP7 People (Marie Curie) Programme, under Grant Agreement No 215840, 2008–2012.

REFERENCES

1. Maher EA, Furnari FB, Bachoo RM et al. Malignant glioma: genetics and biology of a grave matter. *Genes Dev* 2001;15: 1311–33.
2. Furnari FB, Fenton T, Bachoo RM et al. Malignant astrocytic glioma: genetics, biology, and paths to treatment. *Genes Dev* 2007;21:2683–710.
3. Stupp R, Mason WP, Van Den Bent MJ et al. Radiotherapy plus concomitant and adjuvant temozolomide for glioblastoma. *N Engl J Med* 2005;352:987–96.
4. Wen PY, Kesari S. Malignant gliomas in adults. *N Engl J Med* 2008;359:492–507.
5. Van Meir EG, Hadjipanayis CG, Norden AD et al. Exciting new advances in neuro-oncology: the avenue to a cure for malignant glioma. *CA Cancer J Clin* 2010;60:166–93.
6. Hochberg FH, Pruitt A. Assumptions in the radiotherapy of glioblastoma. *Neurology* 1980;30: 907–11.
7. Louis DN, Ohgaki H, Wiestler OD et al. The 2007 WHO classification of tumours of the central nervous system. *Acta Neuropathol* 2007;114:97–109.
8. Chin L, Meyerson M, Aldape E et al. Comprehensive genomic characterization defines human glioblastoma genes and core pathways. *Nature* 2008;455:1061–68.
9. Louis DN, Perry A, Reifenberger G et al. The 2016 World Health Organization classification of tumors of the central nervous system: a summary. *Acta Neuropathol* 2016;131:803–20.
10. Halperin EC. Particle therapy and treatment of cancer. *Lancet Oncol* 2006;7:676–85.

11. Noda SE, El-Jawahri A, Patel D et al. Molecular advances of brain tumors in radiation oncology. *Semin Radiat Oncol* 2009; 19:171–8.
12. O'Rourke DM, Kao GD, Singh N et al. Conversion of a radioresistant phenotype to a more sensitive one by disabling erbB receptor signaling in human cancer cells. *Proc Natl Acad Sci U S A* 1998;95:10842–847.
13. Li B, Yuan M, Kim IA et al. Mutant epidermal growth factor receptor displays increased signaling through the phosphatidylinositol-3 kinase/AKT pathway and promotes radioresistance in cells of astrocytic origin. *Oncogene* 2004;23:4594–602.
14. Halliday J, Helmy K, Pattwell SS et al. *In vivo* radiation response of proneural glioma characterized by protective p53 transcriptional program and proneural–mesenchymal shift. *Proc Natl Acad Sci U S A* 2014;111:5248–53.
15. Stambolic V, MacPherson D, Sas D et al. Regulation of PTEN transcription by p53. *Mol Cell* 2001;8:317–25.
16. Gray LH. Comparative studies of the biological effects of X rays, neutrons and other ionizing radiations. *Br Med Bull* 1946; 4:11–8.
17. Hall EJ, Giaccia AJ. Linear energy transfer and relative biologic effectiveness. In: Hall EJ, Giaccia AJ (eds). *Radiobiology for the Radiologist*. 7th edn. Philadelphia, PA: Lippincott Williams & Wilkins, 2012, 104–13.
18. Held KD, Kawamura H, Kaminuma T et al. Effects of charged particles on human tumor cells. *Front Oncol* 2016;6:128–46.
19. Skarsgard LD. Radiobiology with heavy charged particles: a historical review. *Phys Med* 1998;14:1–19.
20. Short S, Mayes C, Woodcock M et al. Low-dose hypersensitivity in the T98G glioblastoma cell line. *Int J Radiat Biol* 1999;75: 847–55.
21. Short SC, Mitchell SA, Boulton P et al. The response of human glioma cell lines to low-dose radiation exposure. *Int J Radiat Biol* 1999;75:1341–8.
22. Short SC, Kelly J, Mayes CR et al. Low-dose hypersensitivity after fractionated low-dose irradiation *in vitro*. *Int J Radiat Biol* 2001;77:655–64.
23. Short SC, Martindale C, Bourne S et al. DNA repair after irradiation in glioma cells and normal human astrocytes. *Neuro Oncol* 2007;9:404–11.
24. Iwadate Y, Mizoe JE, Osaka Y et al. High linear energy transfer carbon radiation effectively kills cultured glioma cells with either mutant or wild-type p53. *Int J Radiat Oncol Biol Phys* 2001;50: 803–8.
25. Tsuboi K, Tsuchida Y, Nose T et al. Cytotoxic effect of accelerated carbon beams on glioblastoma cell lines with p53 mutation: clonogenic survival and cell-cycle analysis. *Int J Radiat Biol* 1998;74:71–9.
26. Tsuchida Y, Tsuboi K, Ohyama H et al. Cell death induced by high-linear-energy transfer carbon beams in human glioblastoma cell lines. *Brain Tumor Pathol* 1998;15:71–6.
27. Suzuki M, Kase Y, Yamaguchi H et al. Relative biological effectiveness for cell-killing effect on various human cell lines irradiated with heavy-ion medical accelerator in Chiba (HIMAC) carbon-ion beams. *Int J Radiat Oncol Biol Phys* 2000;48:241–50.
28. Tsuboi K, Moritake T, Tsuchida Y et al. Cell cycle checkpoint and apoptosis induction in glioblastoma cells and fibroblasts irradiated with carbon beam. *J Radiat Res* 2007;48:317–25.
29. Combs SE, Bohl J, Elsasser T et al. Radiobiological evaluation and correlation with the local effect model (LEM) of carbon ion radiation therapy and temozolomide in glioblastoma cell lines. *Int J Radiat Biol* 2009;85:126–37.
30. Combs SE, Rieken S, Wick W et al. Prognostic significance of IDH-1 and MGMT in patients with glioblastoma: one step forward, and one step back? *Radiat Oncol* 2011;6:1–5.
31. Linstadt DE, Castro JR, Phillips TL. Neon ion radiotherapy: results of the phase I/II clinical trial. *Int J Radiat Oncol Biol Phys* 1991;20:761–9.
32. Castro JR, Phillips TL, Prados M et al. Neon heavy charged particle radiotherapy of glioblastoma of the brain. *Int J Radiat Oncol Biol Phys* 1997;38: 257–61.
33. Castro JR, Saunders WM, Austin-Seymour MM et al. A phase I–II trial of heavy charged particle irradiation of malignant glioma of the brain: A Northern California oncology group study. *Int J Radiat Oncol Biol Phys* 1985;11:1795–1800.
34. Mizoe JE, Tsujii H, Hasegawa A et al. Phase I/II clinical trial of carbon ion radiotherapy for malignant gliomas: combined X-ray radiotherapy, chemotherapy, and carbon ion radiotherapy. *Int J Radiat Oncol Biol Phys* 2007;69:390–96.
35. Tsujii H, Mizoe J, Kamada T et al. Overview of clinical experiences on carbon ion radiotherapy at NIRS. *Radiother Oncol* 2004;73:S41–9.
36. Combs SE, Nikoghosyan A, Jaekel O et al. Carbon ion radiotherapy for pediatric patients and young adults treated for tumors of the skull base. *Cancer* 2009;115:1348–55.
37. Combs SE, Kieser M, Rieken S et al. Randomized phase II study evaluating a carbon ion boost applied after combined radiochemotherapy with temozolomide versus a proton boost after radiochemotherapy with temozolomide in patients with primary glioblastoma: the CLEOPATRA trial. *BMC Cancer* 2010;10:478.
38. Combs SE, Burkholder I, Edler L et al. Randomised phase I/II study to evaluate carbon ion radiotherapy versus fractionated stereotactic radiotherapy in patients with recurrent or progressive gliomas: the CINDERELLA trial. *BMC Cancer* 2010;10:533.
39. Tsujii H, Mizoe J, Kamada T et al. Clinical Results of Carbon Ion Radiotherapy at NIRS. *J Radiat Res* 2007;48:A1–A13.
40. Furusawa Y, Fukutsu K, Aoki M et al. Inactivation of Aerobic and Hypoxic Cells from Three Different Cell Lines by Accelerated 3He-, 12C-and 20Ne-Ion Beams. *Radiat Res* 2000; 154:485–96.
41. Tsuruoka C, Suzuki M, Kanai T et al. LET and ion species dependence for cell killing in normal human skin fibroblasts. *Radiat Res* 2005;163:494–500.
42. Suzuki M, Tsuruoka C, Kanai T et al. Cellular and molecular effects for mutation induction in normal human cells irradiated with accelerated neon ions. *Mutat Res* 2006;594:86–92.
43. Tsuruoka C, Furusawa Y, Anzai K et al. Rejoining kinetics of G 1-PCC breaks induced by different heavy-ion beams with a similar LET value. *Mutat Res* 2010;701:47–51

44. Liu CH, Kawata T, Zhou GM et al. Comparison of the repair of potentially lethal damage after low-and high-LET radiation exposure, assessed from the kinetics and fidelity of chromosome rejoining in normal human fibroblasts. *J Radiat Res* 2013;54: 989–97.
45. Kanai T, Endo M, Minohara S et al. Biophysical characteristics of HIMAC clinical irradiation system for heavy-ion radiation therapy. *Int J Radiat Oncol Biol Phys* 1999;44:201–10.
46. Torikoshi M, Minohara S, Kanematsu N et al. Irradiation System for HIMAC. *J Radiat Res* 2007;48:A15–25.
47. Matsufuji N, Kohno T, Kanai T. Comprehensive study on the fragment reaction of relativistic heavy charged particles for heavy-ion radiotherapy. *Jpn J Med Phys* 1999;61:230–32 (in Japanese).
48. Joiner MC, Marples B, Lambin P et al. Low-dose hypersensitivity: current status and possible mechanisms. *Int J Radiat Oncol Biol Phys* 2001;49:379–89.
49. Fertil B, Malaise EP. Inherent cellular radiosensitivity as a basic concept for human tumor radiotherapy. *Int J Radiat Oncol Biol Phys* 1981;7:621–29.
50. Sørensen BS, Overgaard J, Bassler N. *In vitro* RBE-LET dependence for multiple particle types. *Acta Oncol* 2011;50: 757–62.
51. Weyrather WK, Ritter S, Scholz M et al. RBE for carbon track-segment irradiation in cell lines of differing repair capacity. *Int J Radiat Biol* 1999;75:1357–364.
52. Jones B. A simpler energy transfer efficiency model to predict relative biological effect for protons and heavier ions. *Front Oncol* 2015;5:184.
53. Jones B. Corrigendum: a simpler energy transfer efficiency model to predict relative biological effect for protons and heavier ions. *Front Oncol* 2016;6:184
54. Tobias CA, Blakely EA, Chang PY et al. Response of sensitive human ataxia and resistant T-1 cell lines to accelerated heavy ions. *Br J Cancer Suppl* 1984;6:175–85.
55. Katz R, Ackerson B, Homayoonfar M et al. Inactivation of cells by heavy ion bombardment. *Radiat Res* 1971;47:402–25.
56. Suzuki M, Watanabe M, Kanai T et al. LET dependence of cell death, mutation induction and chromatin damage in human cells irradiated with accelerated carbon ions. *Adv Space Res* 1996;18:127–36.
57. Chatterjee A, Schaefer HJ. Microdosimetric structure of heavy ion tracks in tissue. *Radiat Environ Biophys* 1976;13:215–27.
58. Kleihues P, Ohgaki H. Phenotype vs genotype in the evolution of astrocytic brain tumors. *Toxicol Pathol* 2000;28:164–70.
59. Ino Y, Betensky RA, Zlatescu MC et al. Molecular subtypes of anaplastic oligodendroglioma. *Clin Cancer Res* 2001;7:839–45.